

# (Glyco)sphingolipids are sorted in sub-apical compartments in HepG2 cells

van IJzendoorn, S. C. D.; Hoekstra, D.

*Published in:*
Journal of Cell Biology

*DOI:*
10.1083/jcb.142.3.683



*Publication date:*
1998

# (Glyco)sphingolipids Are Sorted in Sub-Apical Compartments in HepG2 Cells: A Role for Non-Golgi–Related Intracellular Sites in the Polarized Distribution of (Glyco)sphingolipids

**Sven C.D. van IJzendoorn and Dick Hoekstra**

Department of Physiological Chemistry, Faculty of Medical Sciences, University of Groningen, Groningen, The Netherlands

***Abstract.*** In polarized HepG2 cells, the fluorescent sphingolipid analogues of glucosylceramide ($C_6$-NBD-GlcCer) and sphingomyelin ($C_6$-NBD-SM) display a preferential localization at the apical and basolateral domain, respectively, which is expressed during apical to basolateral transcytosis of the lipids (van IJzendoorn, S.C.D., M.M.P. Zegers, J.W. Kok, and D. Hoekstra. 1997. *J. Cell Biol.* 137:347–457). In the present study we have identified a non-Golgi–related, sub-apical compartment (SAC), in which sorting of the lipids occurs. Thus, in the apical to basolateral transcytotic pathway both $C_6$-NBD-GlcCer and $C_6$-NBD-SM accumulate in SAC at 18°C. At this temperature, transcytosing IgA also accumulates, and colocalizes with the lipids. Upon rewarming the cells to 37°C, the lipids are transported from the SAC to their preferred membrane domain. Kinetic evidence is presented that shows in a direct manner that after leaving SAC, sphingomyelin disappears from the apical region of the cell, whereas GlcCer is transferred to the apical, bile canalicular membrane. The sorting event is very specific, as the GlcCer epimer $C_6$-NBD-galactosylceramide, like $C_6$-NBD-SM, is sorted in the SAC and directed to the basolateral surface. It is demonstrated that transport of the lipids to and from SAC is accomplished by a vesicular mechanism, and is in part microtubule dependent. Furthermore, the SAC in HepG2 bear analogy to the apical recycling compartments, previously described in MDCK cells. However, in contrast to the latter, the structural integrity of SAC does not depend on an intact microtubule system. Taken together, we have identified a non-Golgi–related compartment, acting as a "traffic center" in apical to basolateral trafficking and vice versa, and directing the polarized distribution of sphingolipids in hepatic cells.

Key words: sphingolipid • immunoglobulin A • sorting • transcytosis • HepG2 cell

The plasma membrane (PM)[1] of polarized cells is divided into a basolateral and an apical PM domain. Each membrane domain has its specific protein and lipid composition, an essential feature for the polarized function of these cells. To generate and maintain such unique membrane compositions, proteins and lipids have to be sorted and targeted to the appropriate PM domains. In polarized cells apical delivery may occur via two routes, including a direct transport from the TGN, and an indirect pathway, in which before apical delivery, newly synthesized components are first transported from the TGN to the basolateral surface. Subsequently, apical constituents are endocytosed, sorted into transcytotic vesicles, and transported to the apical pole of the cell. To add to the complexity of trafficking in polarized cells, proteins, and lipids from each membrane domain are continuously reinternalized, recycled, or redistributed, reflecting a dynamic equilibrium indispensable for maintaining a dynamic membrane composition capable of adapting to different needs. As a consequence, apical (and basolateral) components must be sorted into or excluded from vesicles with preferential targets at various intracellular sites, each site thus contributing to the polarized distribution of PM components.

For both proteins and distinct (glyco)sphingolipids, the main intracellular sorting site for polarized transport is believed to be the TGN. Specifically, in this compartment,

Address all correspondence to Dick Hoekstra, Department of Physiological Chemistry, University of Groningen, A. Deusinglaan 1, 9713 AV, Groningen, The Netherlands. Tel.: +31-50-3632741. Fax: +31-50-3632728. E-mail: d.hoekstra@med.rug.nl

1. *Abbreviations used in this paper*: ARC, apical recycling compartment; BC, bile canaliculus; BCP, bile canalicular pole; GalCer, galactosylceramide; GlcCer, glucosylceramide; GSL, glycosphingolipid; pIgR, polymeric immunoglobulin receptor; PM, plasma membrane; SAC, sub-apical compartments; SM, sphingomyelin; TxR, Texas red–labeled.

several apical proteins appear to associate with glycosphingolipid (GSL)-enriched domains (Brown and Rose, 1992), so-called GSL rafts (Simons and Ikonen, 1997). Budding of these rafts will give rise to vesicles, with an apical destination (Simons and Wandinger-Ness, 1990). Whereas MDCK cells predominantly use the direct pathway for the delivery of apical components (Matlin and Simons, 1984; Misek et al., 1984; Pfeiffer et al., 1985; Simons and Fuller, 1985), other polarized cells may use a combination of the direct and the indirect, transcytotic pathway (van't Hof and van Meer, 1990; Weimbs et al., 1997). Hepatic cells are believed to rely mainly on the indirect, transcytotic pathway for the apical delivery of newly synthesized proteins (Bartles et al., 1987; Cariappa and Kilberg, 1992; Schell et al., 1992), although evidence is accumulating which indicates that direct Golgi to apical transport of proteins and lipids also occurs (Ali and Evans, 1990; Zaal et al., 1993; Zegers and Hoekstra, 1997). The overall mechanism involved in the apical flow of proteins and lipids via the indirect, transcytotic route is still largely unclear. For example, whether GSL-rafting plays a role in this route remains to be determined.

To study transcytosis, the polymeric immunoglobulin receptor (pIgR) and its ligand IgA is often used as a marker of this pathway (Mostov and Deitcher, 1986; Apodaca et al., 1991; Mostov et al., 1995). It has thus been demonstrated that transcytosis proceeds along routes, which constitute part of other pathways used by non-transcytosing molecules. pIgR-IgA complexes, endocytosed from the basolateral surface, are delivered to basolateral endosomes and reach via transcytosis sub-apical endosomal compartments, termed apical recycling compartments (ARC) in MDCK cells, before their delivery to the apical PM (Apodaca et al., 1994; Barroso and Sztul, 1994). Other apical proteins such as dipeptidyl peptidase IV and the glycosylphosphatidylinositol-anchored protein 5′ nucleotidase have been suggested to use the same transcytotic pathway as pIgR–IgA (Barr et al., 1995). As revealed in MDCK cells, the sub-apical compartments (SAC) are not only accessible to proteins with a preference for apical localization. Also a considerable portion of the basolaterally endocytosed transferrin receptor was found to be transported to the apical recycling compartment. However, in contrast to the apically targeted pIgR-IgA, the transferrin receptor returns to the basolateral surface (Apodaca et al., 1994). Hence, these data suggest a role for the sub-apical compartment in the generation and/or maintenance of the polarized distribution of PM components.

Previous studies in MDCK (van Genderen and van Meer, 1995) and the human hepatoma–derived cell line, HepG2 (van IJzendoorn et al., 1997; Zegers and Hoekstra, 1997) revealed that sphingolipids such as glucosylceramide (GlcCer) and sphingomyelin (SM) also use the transcytotic pathway to traverse the cell in either direction. However, very little is known of the mechanisms involved in transcytotic transport of lipids. In a recent study, we demonstrated that in well-polarized HepG2 cells fluorescent acyl chain–labeled analogues of glucosylceramide ($C_6$-NBD-GlcCer) and sphingomyelin ($C_6$-NBD-SM) are segregated in the apical to basolateral transcytotic pathway (van IJzendoorn et al., 1997). The observed segregation event did not involve the Golgi apparatus, hinting at the existence of another, yet unidentified subcellular compartment where sphingolipids are sorted. In the present work we provide evidence that SAC, similar to ARC as defined in MDCK cells, are also operative in HepG2 cells. Specifically, it is demonstrated that these SAC represent the major intracellular site in the transcytotic pathway where GlcCer and SM are sorted and directed to distinct PM domains.

## Materials and Methods

### Materials

Sphingosylphosphorylcholine, 1-β-glucosylsphingosine, cerebroside type II, asialofetuin type I, and geneticin (G-418) were from Sigma Chemical Co. (St. Louis, MO). Albumin (from bovine serum, fraction V) was bought from Fluka Chemie AG (Buchs, Switzerland). 6-(*N*-[7-nitrobenz-2-oxa-1,3-diazol-4-yl]amino) hexanoic acid ($C_6$-NBD) was obtained from Molecular Probes (Eugene, OR). DME was purchased from GIBCO-BRL (Paisley, Scotland). FCS was bought from BioWhittaker (Verviers, Belgium), and $Na_2S_2O_4$ was from Merck (Darmstadt, Germany). Nocodazole was obtained from Boehringer Mannheim (Mannheim, Germany). PSC 833 and MK 571 were gifts from Dr. E. Vellenga (University of Groningen, The Netherlands). Texas red–labeled IgA was kindly provided by Dr. K. Dunn (Indiana University Medical Center, Indianapolis, IN). pIgR cDNA and an mAb against pIgR was kindly provided by Dr. K. Mostov (University of California, San Francisco, CA). All other chemicals were of analytical grade.

### Cell Culture

HepG2 cells were grown at 37°C under a 5% $CO_2$-containing, humidified atmosphere in DME, supplemented with 10% heat-inactivated (at 56°C) FCS, 2 mM L-glutamine, 100 IU/ml penicillin, and 100 μg/ml streptomycin. Medium was replaced every other day. For experiments, cells were used 3 d after plating. At this time the cells had reached an optimal ratio of polarity versus density, i.e., No. of bile canalicular spaces (BCs) versus No. of cells.

### Synthesis of $C_6$-NBD–labeled Sphingolipids

$C_6$-NBD-GlcCer and $C_6$-NBD-SM were synthesized from $C_6$-NBD and 1-β-glucosylsphingosine and sphingosylphosphorylcholine, respectively, as described elsewhere (Kishimoto, 1975; Babia et al., 1994). 1-β-D-galactosylceramide was prepared from cerebroside (type II) (Goda et al., 1987). The $C_6$-NBD-lipids were stored at −20°C and routinely checked for purity.

### Cell Labeling and Lipid Transport Assays

For microscopy, cells were plated onto glass coverslips. For biochemical analysis cells were cultured in 25-$cm^2$ culture flasks (Costar, Cambridge, UK). After 3 d, cells were washed three times with a PBS solution. $C_6$-NBD-GlcCer or $C_6$-NBD-SM were dried under nitrogen, redissolved in absolute ethanol, and then injected into HBSS under vigorous vortexing. The final concentration of ethanol was kept below 0.5% (vol/vol). Cells were incubated with 4 μM of either lipid analogue at 37°C for 30 min (see Fig. 1, *step 1*). To monitor transport of apical membrane–associated lipid analogues, the basolateral pool of fluorescent lipid analogues was depleted by incubating the cells in HBSS, supplemented with 5% (wt/vol) BSA at 4°C twice for 30 min (back exchange, Fig. 1, *step 2*). Then, cells were washed three times with ice-cold PBS, rewarmed to the desired temperature, and then incubated in HBSS, with 5% (wt/vol) BSA (Fig. 1, *step 3*). The 18°C temperature block was dictated by previous observations in MDCK cells showing that an incubation at this temperature causes a selective inhibition of transcytotic transport, as revealed by the accumulation of the transcytotic marker pIgA-R (Apodaca et al., 1994; Barosso and Sztul, 1994). In some experiments, NBD fluorescence associated with BC was eliminated by incubating the cells with 30 mM sodiumdithionite (diluted from a stock solution of 1 M $Na_2S_2O_4$ in 1 M Tris, pH 10) at 4°C for 7 min (Fig. 1, *step 4*). As described previously, sodiumdithionite is able to pass the tight junctional complexes in HepG2 cells (van IJzendoorn et al.,

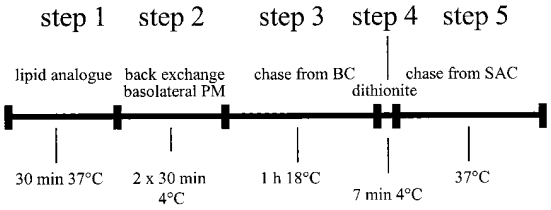


*Figure 1.* Schematic representation of the various steps of the lipid transport assays. Cells are incubated with $C_6$-NBD-lipids at 37°C for 30 min, causing labeling of both apical (*BC*) and basolateral membranes (*step 1*). Subsequently, the fraction of the fluorescent lipid analogue residing at the basolateral PM is depleted by BSA at 4°C twice for 30 min (*step 2*). The BC-associated lipid analogue is then chased into sub-apical compartments (see Results) at 18°C for 1 h in BSA-containing medium (*step 3*). The presence of BSA in the medium during this step will prevent reentry of any lipid analogue that might arrive basolaterally during the chase. Next, the NBD-labeled lipid remaining at the BC is quenched by sodiumdithonite (*step 4*), after which transport of the sub-apically derived lipid analogue can be monitored upon rewarming and incubating the cells at 37°C (*step 5*). The vertical bar in between each step represents wash steps.

1997), whereas BSA does not affect the labeling of BC (see Results; compare with van IJzendoorn et al., 1997). Sodiumdithionite-treated cells were then washed extensively (>10 times) with ice-cold HBSS, after which transport was re-activated by rewarming and further incubating the cells in HBSS at 37°C (Fig. 1, *step 5*). BSA (5% wt/vol) was included in the medium to prevent the lipid analogues from re-entering the cells at the basolateral surface. After all final incubations, cells were washed with ice-cold HBSS and kept on ice until use (within 30 min).

To study the involvement of microtubules on transport of BC-associated lipids, nocodazole (33 μM, diluted from a 10 mM stock solution) was added during step 2 of the incubation scheme depicted in Fig. 1 and kept present in all subsequent steps. In parallel experiments, cells were treated with 33 μM nocodazole at 4°C for 1 h after the 18°C chase of BC-associated lipid analogues (Fig. 1, *step 3*). Indirect immunofluorescence, using a mAb directed against fl-tubulin (Sigma Chemical Co.), was performed to verify the microtubule-disrupting potency of nocodazole in HepG2 cells (not shown).

To study the effect of PSC 833 and MK 571, which are specific inhibitors of the multi-drug resistance proteins MDR1/*P*-glycoprotein and MRP1, respectively, on the different transport steps, cells were incubated with MK 571 (25 μM) or PSC 833 (5 μg/ml) before step 1, with either inhibitor between steps 2 and 3, or between steps 4 and 5. The concentration of PSC 833 was sufficient to completely block the excretion of rhodamine 123 into BC of HepG2 cells by MDR1/*P*-glycoprotein activity (not shown).

### *Quantification of Fluorescent BC Labeling*

As a measure for transport of the lipid analogues to and from the BC membranes, the percentage of NBD-positive BC membranes was determined as described elsewhere (van IJzendoorn et al., 1997). In brief, BC were first identified by phase contrast illumination, and then classified as NBD-positive or NBD-negative under epifluorescence illumination. Furthermore, distinct pools of fluorescence are discerned, present in vesicular structures adjacent to BC, which in this work are defined as SAC. Together, BC and SAC thus constitute the apical, bile canalicular pole (BCP) in HepG2 cells. Therefore, within the BCP region the localization of the fluorescent lipid analogues will be defined as being derived from BC, SAC, or both. For this kind of quantification, at least 50 BCP were analyzed per coverslip. All data are expressed as the mean ± SD of four independent experiments, carried out in duplicate.

### *Lipid Extraction and Quantification*

Lipids were extracted according to the method of Bligh and Dyer (1959) and analyzed by thin layer chromatography using $CHCl_3$/methanol/$NH_4OH$/$H_2O$ (35:15:2:0.5, vol/vol/vol/vol) as running solvent. For quantification, fluorescent lipids were scraped from the TLC plates, followed by vigorous shaking in 1% (vol/vol) Triton X-100 in $H_2O$ for 60 min to remove the lipids from the silica. Silica particles were then spun down and NBD fluorescence was measured spectrophotometrically in an SLM fluorometer at excitation and emission wavelengths of 465 nm and 530 nm, respectively.

### *Transfection of HepG2 Cells with the pIgR*

HepG2 cells were plated at low density (±20% confluency) in medium, containing 20% FCS. Cells were allowed to attach and spread for 24 h. The cells were then transfected with the cDNA encoding wild-type rabbit pIgR, inserted into a pCB6 expression vector, which contained a neomycin resistance marker. The synthetic pyridinium-based amphiphile SAINT-2 (a gift from Saint BV, Groningen, The Netherlands) was used as DNA carrier. Preparation of small unilamellar SAINT-2/dioleylphosphatidyl ethanolamine (DOPE) vesicles and transfection was performed as described by van der Woude et al. (1997). Cells were selected in culture media, supplemented with 600 μg/ml geneticin (G-418). Successful transfection of HepG2 cells was evidenced by indirect immunofluorescence microscopy using a mAb against pIgR, and by the ability of the cells to internalize Texas red–labeled IgA (TxR-IgA) in the presence of a 100-fold excess asialofetuin (see Results). The polarity of the transfected cells was verified by determination of the ratio BC/cells (Zegers and Hoekstra, 1997).

### *Internalization of Texas Red–labeled IgA*

Cells transfected with the pIgR as described above were washed and asialoglycoprotein receptors were saturated with excess asialofetuin at 37°C for 30 min to prevent uptake of IgA via these receptors (see Results). Cells were incubated with TxR-IgA (50 μg/ml) at 4°C for 30 min. Cells were then washed to remove non-bound TxR-IgA and further incubated at 18°, 37°C, or a combination of both for various time intervals, depending on the experiment.

### *Microscopical Analysis and Image Processing*

Cells were examined microscopically using a conventional Olympus Provis AX70 fluorescence microscope. Photomicrographs were taken using Illford HP5-plus films and scanned. For confocal laser scanning microscopy a TCS Leica (Heidelberg, Germany) apparatus equipped with a argon/krypton laser coupled to a Leitz DM IRB-inverted microscope was used. All images were converted to tagged-information-file format before printing on a Fujix P3000 printer.

## *Results*

### *Apical Membrane–derived $C_6$-NBD-GlcCer and $C_6$-NBD-SM Are Delivered to SAC*

In a previous study we demonstrated that $C_6$-NBD-GlcCer and $C_6$-NBD-SM display a preferential apical and basolateral localization, respectively, in HepG2 cells. This preferential localization was established during apical to basolateral transcytosis, a novel pathway in hepatic cells. A tentative role for non-Golgi–related SAC in the apical recycling of $C_6$-NBD-GlcCer was proposed (van IJzendoorn et al., 1997). However, neither the identity of these compartments nor their functional involvement in the apical to basolateral transcytotic pathway of either lipid was established. To address these issues, the following experiments were performed.

Cells were labeled with 4 μM $C_6$-NBD-SM or $C_6$-NBD-GlcCer at 37°C for 30 min. In this way, >70% of the BC, identified by phase-contrast microscopy, became labeled, the lipid analogues thus becoming inserted into the canalicular membrane. In addition, fluorescently labeled vesicular structures are observed in the cytoplasm, presumably representing compartments of the endocytic internalization pathway and transport vesicles still en route to their

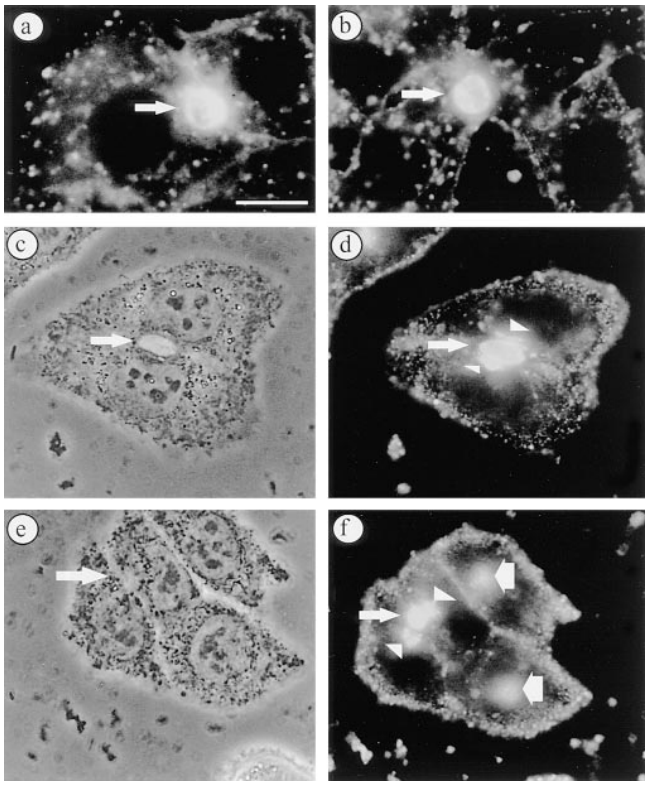


*Figure 2.* BC-derived $C_6$-NBD-GlcCer and $C_6$-NBD-SM accumulate in SAC at 18°C. Cells were labeled with 4 μM $C_6$-NBD-GlcCer or $C_6$-NBD-SM at 37°C for 30 min. Subsequently, the fluorescent lipid pool in the basolateral PM was removed by back exchange (*a*, $C_6$-NBD-SM; *b*, $C_6$-NBD-GlcCer; *arrows* point to BC). Alternatively, the cells were subsequently washed and further incubated at 18°C for 60 min. $C_6$-NBD-SM (*c* and *d*) and $C_6$-NBD-GlcCer (*e* and *f*) labeled the BCP of the cells, i.e., BC (*thin arrows*) and vesicular structures located near the BC membranes (*arrowheads*). In cells that did not participate in the formation of BC some accumulation of the fluorescent lipid analogue in juxtanuclear compartments was often seen (*f*, *wide arrows*) (*c* and *e*, phase contrast to *d* and *f*, respectively). Bar, 10 μm.

target membranes. (Fig. 2, *a* and *b*; compare with Fig. 2 in van IJzendoorn et al., 1997). To subsequently monitor the fate of the apical membrane–associated lipid analogues, the basolateral pool was depleted by incubating the cells in HBSS, supplemented with 5% BSA at 4°C twice for 30 min (back exchange). The cells were then washed, rewarmed to either 18° (see Materials and Methods) or 37°C, and further incubated in HBSS, supplemented with 5% BSA, for 60 min. At 18°C, basolateral delivery of the lipid analogues, relative to that at 37°C, was inhibited by ~70%, as calculated from the amount of $C_6$-NBD-SM and $C_6$-NBD-GlcCer that could be retrieved in the BSA-containing medium. Fluorescence microscopical analysis revealed that upon chasing BC-associated lipid analogues at 18°C, a major part of both $C_6$-NBD-GlcCer and $C_6$-NBD-SM remained localized at the BCP of the cells, i.e., in BC and/or sub-apically located vesicular structures (Fig. 2, *d* and *f*: *thin arrows*, BC; *arrowheads*, SAC). To reveal a net directional movement of the lipid analogues in the apical bile canalicular area, BCP labeling was distinguished into labeling of only BC, only SAC or labeling of both BC and SAC. (See Materials and Methods, and Figs. 2, *a* [BC] and *f* [BC + SAC]; 4 *b* [SAC].) Such semi-quantitative analysis of labeling of the apical region revealed that before the chase, >90% of the label detected in the BCP region, was found to be solely associated with BC (Fig. 3 *A*; see also the labeling pattern in Fig. 2, *a* and *b*). Thus, the prominent labeling of sub-apical structures, as revealed by accumulation of the lipid analogues, was not observed before the chase at 18°C was started (also compare with van IJzendoorn et al., 1997). After the 18°C chase, the majority (±85%) of the $C_6$-NBD-GlcCer or $C_6$-NBD-SM present in the BCP was associated with both SAC and BC (Fig. 3 *B*, *BC + SAC* and *SAC*), while only ~15% was due to the exclusive labeling of BC only (Fig. 3 *B*, *BC*). Also note that, for either lipid analogue, the percentage of labeled BCP did not change during the chase. In conjunction with the fact that the presence of BSA in the incubation medium prevented potential re-internalization of the lipid analogues from the basolateral surface and subsequent transport to the SAC, the data thus indicate that the lipid analogues were transported via a direct (i.e., basolateral membrane–independent) route from BC to SAC.

Not all cells participate in the formation of BC (Zegers and Hoekstra, 1997). Remarkably, however, also in cells lacking a distinct apical PM domain a significant part of the intracellular $C_6$-NBD-GlcCer and $C_6$-NBD-SM fractions accumulated in juxtanuclear compartments after a

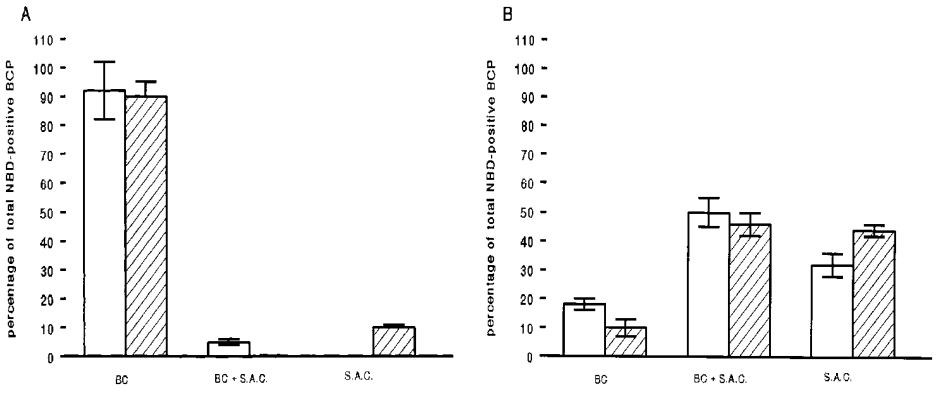


*Figure 3.* Semi-quantitative analysis of BCP labeling: accumulation of $C_6$-NBD-lipid analogues in SAC. Cells were labeled and treated as depicted in Fig. 1. *A* represents the distribution of NBD lipid in BC and SAC after step 1 (30 min at 37°C) while the distribution indicated in *B* was obtained after a subsequent back exchange and chase from BC at 18°C for 60 min (Fig. 1, *step 2* and *3*). In both cases, the percentage $C_6$-NBD-GlcCer- and $C_6$-NBD-SM-labeled BCP was ~85%. Labeling of BCP was distinguished in either NBD-positive BC only, a cellular BCP fraction in which both BC and SAC were labeled (*BC + SAC*), or NBD-positive SAC. Data are expressed as percentage of the total number of $C_6$-NBD-GlcCer– (*white bars*) and $C_6$-NBD-SM–positive (*hatched bars*) BCP (minimum of 50/coverslip; mean ± SEM) of at least four independent experiments carried out in duplicate.

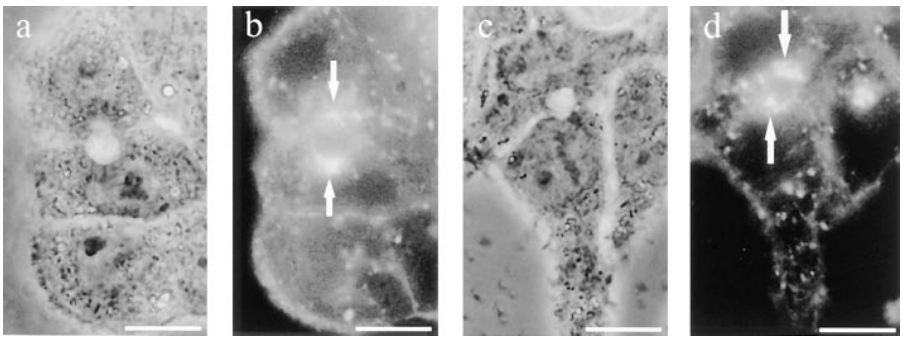


*Figure 4.* Sodiumdithionite reduces BC-associated fluorescence without getting access to SAC. Cells were labeled with 4 μM $C_6$-NBD-GlcCer or $C_6$-NBD-SM at 37°C for 30 min. The fluorescent lipid analogues present in the basolateral PM were then depleted by incubating the cells twice for 30 min in HBBS, supplemented with 5% BSA at 4°C. Cells were subsequently washed with PBS, rewarmed, and then incubated at 18°C in HBSS + BSA for 1 h. When the cells were subsequently treated with 30 mM sodiumdithionite in HBSS (diluted from a 1 M stock solution in 1 M Tris/HCl, pH 10) at 4°C for 7 min, $C_6$-NBD-GlcCer (*b*; *a*, phase contrast to *b*) and $C_6$-NBD-SM (*d*; *c*, phase contrast to *d*) were absent from BC, while leaving the fluorescence in sub-apical structures unaltered (*arrows*). Bar, 10 μm.

60-min incubation at 18°C (Fig. 2 *f*, *wide arrows*), but not at 37°C (data not shown).

Finally, it is important to note that in the experiments at both 18° and 37°C, the only fluorescent lipid analogue identified in the incubation media and cell fractions was the one that was exogenously administered, indicating that no metabolism of either lipid had occurred during the time span of the experiments (data not shown). Taken together, the data clearly demonstrate that low temperature (18°C) can selectively impede apical to basolateral transcytosis of both $C_6$-NBD-GlcCer and $C_6$-NBD-SM. The observed accumulation of the analogues in the same subcellular compartments (SAC) located adjacent to the BC membrane, indicates that at least early in the trafficking pathway during apical to basolateral transcytosis, both $C_6$-NBD-GlcCer and $C_6$-NBD-SM pass through the same compartments, while before their arrival in SAC, significant sorting, proceeding their preferential rerouting to apical and basolateral region, respectively, has not yet occurred. The latter is supported by the striking similarity in semiquantitative distribution of the two analogues (Fig. 3 *B*).

### *$C_6$-NBD-SM and $C_6$-NBD-GlcCer Flow from SAC to Distinct PM Domains*

Since GlcCer and SM display a distinct preferential localization within the cell, we next examined the possibility as to whether the compartments identified as SAC by accumulation of either lipid analogue, were functionally involved in redirecting their trafficking. Hence, to address the issue of SAC acting as a sorting compartment, the cells were labeled with $C_6$-NBD-GlcCer or $C_6$-NBD-SM, similarly as described above. After chasing the lipid analogues into SAC at 18°C, NBD fluorescence still present in the BC was irreversibly abolished by incubating the cells with 30 mM sodiumdithionite at 4°C for 10 min (Fig. 4; see Materials and Methods). After treatment, ~80–90% of the identified BCP was still fluorescently labeled (Fig. 5 *A*), but <10% of the total fluorescence ($C_6$-NBD-GlcCer or $C_6$-NBD-SM) located in the bile canalicular area after dithionite quenching, was due to labeling of BC (Fig. 5, *B* and *C*, *0 min*; for fluorescence images compare Fig. 4, *b*/*d* vs. Fig. 2, *b*/*d*). Indeed, dithionite effectively abolishes NBD fluorescence appearing at the luminal surface of the bile canalicular space, while it does not gain access to intracellular sites at the conditions of the treatment (van IJzendoorn et al., 1997). Consequently, labeling with the lipid analogues was predominantly in SAC alone (Fig. 4), representing >80% of the NBD-positive BCP fraction (Fig. 5, *B* and *C*, *SAC*).

The virtually exclusive labeling of SAC in the BCP region, as accomplished by this treatment thus allowed us, after extensive washing of the cells to remove the dithionite, to investigate the subsequent fate of $C_6$-NBD-GlcCer and $C_6$-NBD-SM associated with the SAC. To this end, transport was re-activated by rewarming and further incubating the cells in HBSS at 37°C for various time intervals. BSA was included in the medium to prevent re-internalization of the lipid analogues from the basolateral PM and subsequent basolateral to apical transcytosis. Over a 30-min time span, the percentage of BCP labeled with $C_6$-NBD-GlcCer remained fairly constant at ~90%, whereas the percentage of $C_6$-NBD-SM–labeled BCP decreased to ±55% after 30 min (Fig. 5 *A*). Thus, after re-activation of transport, $C_6$-NBD-SM, in contrast to $C_6$-NBD-GlcCer, disappeared from the apical membrane region. Indeed, while after a 30-min time interval the localization of the remaining fraction of $C_6$-NBD-GlcCer in the BCP compartments was about equally distributed between BC and SAC (Fig. 5 *B*), <25% of the remaining fraction of the $C_6$-NBD-SM fluorescence at the BCP was associated with BC. Rather, nearly 80% was found to be associated with SAC over the entire 30-min time interval (Fig. 5 *C*). From these data we conclude that after re-activation of transport of the lipid analogues from the SAC, $C_6$-NBD-SM trafficking prefers a sub-apical to basolateral direction, while $C_6$-NBD-GlcCer recycles from the SAC to BC thus remaining in the apical region of the cell. Hence, the results suggest that in the sub-apical vesicular structures $C_6$-NBD-GlcCer and $C_6$-NBD-SM are sorted and flow preferentially to the apical and basolateral membrane domains, respectively.

### *Sorting of Glycosphingolipid in SAC Is Highly Specific*

To further determine the specificity of the sorting event in the SAC, the trafficking of $C_6$-NBD-GalCer was examined. Whereas $C_6$-NBD-GlcCer and $C_6$-NBD-SM have entirely different head groups (glucose versus phosphocholine, respectively), $C_6$-NBD-GlcCer and $C_6$-NBD-GalCer are epimers (i.e., they differ in the spatial orientation of only one hydroxyl moiety in the carbohydrate head group). To label the bile canalicular membrane, the cells were labeled with $C_6$-NBD-GalCer at 37°C for 30 min and back exchanged (according to Fig. 1, *step 1* and *2*). $C_6$-

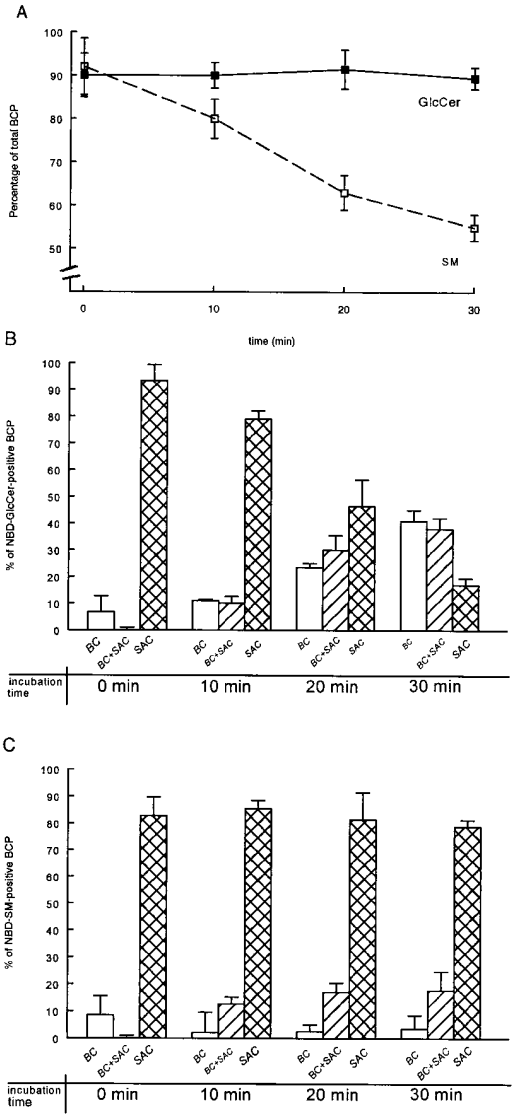


*Figure 5.* Semi-quantitative kinetic analysis of $C_6$-NBD-GlcCer and $C_6$-NBD-SM, exiting from SAC. First, the lipid analogues were accumulated in SAC. To this end, cells were labeled with 4 μM $C_6$-NBD-GlcCer or $C_6$-NBD-SM at 37°C for 30 min. After depletion of the fluorescent lipids from the basolateral PM by back exchange, the cells were subsequently incubated in HBSS + BSA at 18°C for 60 min. To eliminate BC-associated NBD fluorescence, cells were then treated with 30 mM sodiumdithionite at 4°C for 7 min. After removal of the sodiumdithionite by extensive washing, the temperature was shifted to 37°C to reactivate transport from SAC. In *A*, the percentage of BCP labeled with either lipid analogue after a 0- (i.e., before the chase), 10-, 20-, and 30-min chase is presented. In *B*, the distribution of the BCP-associated $C_6$-NBD-GlcCer is shown, and in *C*, that of $C_6$-NBD-SM fluorescence, as determined after the indicated incubation time at 37°C. In *A*, data are expressed as percentage of total (i.e., NBD-positive + NBD-negative) BCP (mean ± SEM) of at least four independent experiments carried out in duplicate. In *B* and *C*, data are expressed as percentage of total NBD-positive BCP (mean ± SEM) of at least four independent experiments, carried out in duplicate.

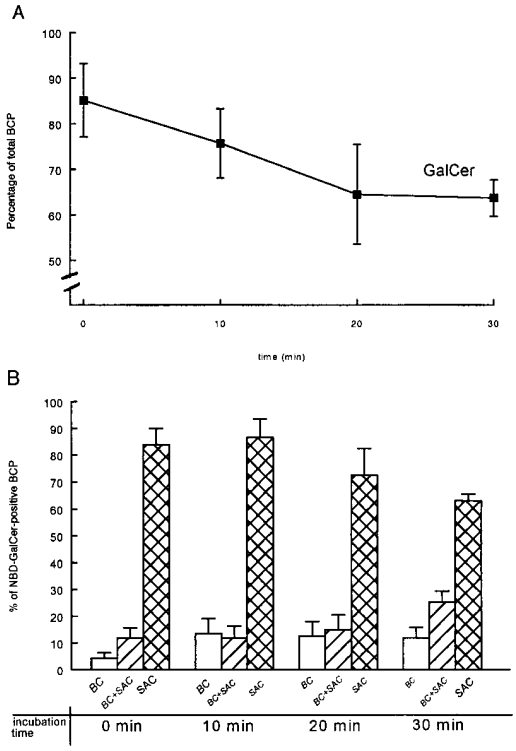


*Figure 6.* Semi-quantitative kinetic analysis of $C_6$-NBD-GalCer, exiting from SAC. The analogue was accumulated in SAC as follows. Cells were labeled with 4 μM $C_6$-NBD-GalCer at 37°C for 30 min to label BC. After depletion of fluorescent lipids from the basolateral PM, the cells were subsequently incubated in HBSS + BSA at 18°C for 60 min. Cells were then treated with 30 mM sodiumdithionite at 4°C for 7 min to eliminate BC-associated fluorescence. After removal of the sodiumdithionite by extensive washing, the temperature was shifted to 37°C to reactivate transport from SAC. In A, the percentage of BCP labeled with $C_6$-NBD-GalCer after a 0, 10, 20 and 30 min chase is presented. In *B*, the distribution of the BCP-associated $C_6$-NBD-GalCer is shown. In *A* and *B*, data are expressed as percentage of total (i.e., NBD-positive + NBD-negative) BCP (mean ± SEM) and of total NBD-positive BCP of at least four independent experiments carried out in duplicate, respectively.

NBD-GalCer was found to be transcytosed to the BC with similar kinetics as those of the short chain analogues of GlcCer and SM (not shown), implying bulk membrane transport. BC-associated $C_6$-NBD-GalCer (±85% of the NBD-positive BCP was due to labeling of only BC) was subsequently chased at 18°C for 60 min in BSA-containing HBSS (Fig. 1, *step 3*). Similar to $C_6$-NBD-GlcCer and -SM, $C_6$-NBD-GalCer was found to accumulate in SAC (not shown). Cells were then subjected to steps 4 and 5 of the incubation scheme (Fig. 1) to examine the exiting of the lipid analogue from the SAC. Over a 30-min time interval, the percentage of $C_6$-NBD-GalCer–labeled BCP decreased from 85% to 65% (Fig. 6 *A*). Compared with the trafficking of $C_6$-NBD-GlcCer and $C_6$-NBD-SM (compare with Fig. 5), $C_6$-NBD-GalCer thus appeared to disappear from the BCP, similarly as observed in the case of $C_6$-NBD-SM. Consistently, as reported previously for the latter analogue, GalCer also preferentially locates to the basolateral membrane, as revealed by fluorescence microscopy (not shown; compare with Fig. 3 in van IJzendoorn et al., 1997). Examination of the distribution of the remaining fraction of $C_6$-NBD-GalCer in the apical area revealed, that the vast majority (60–70%) of this fraction resided exclusively in SAC (Fig. 6 *B*), indicative of a lack of a sub-

stantial movement of $C_6$-NBD-GalCer toward BC, similarly as observed for the SM analogue, and emphasizing that like $C_6$-NBD-SM, the glycolipid, after exiting SAC, disappeared from the apical region of the cell. Hence, the data indicate that $C_6$-NBD-GalCer, like $C_6$-NBD-SM, is preferentially targeted from the SAC to the basolateral PM domain and, thus, appears to be sorted in this compartment from $C_6$-NBD-GlcCer.

### *Sorting at the Luminal Leaflet of SAC; Transcytotic Trafficking of $C_6$-NBD-SM and $C_6$-NBD-GlcCer Occurs by Vesicular Means*

To further define the exclusiveness and specificity of SAC in lipid sorting in the reverse transcytotic pathway in HepG2 cells, it is important to establish the mechanism of trafficking of both sphingolipids in HepG2 cells. This mechanism could involve monomeric flow or vesicle-mediated transport or both. Monomeric flow could entail flip-flop mechanisms across basolateral and apical membranes, mediated by the translocating activities (in outward direction) of MRP1 and MDR1, respectively (van Helvoort et al., 1996; Roelofsen et al., 1997). The evidence indicates that the lipid pool, derived from the apical membrane and arriving in SAC is derived from the exoplasmic leaflet of the apical membrane. Thus, treatment of the cells before the incubation with the lipid analogues (Fig. 1, *step 1*) with the MDR1 inhibitor PSC 833, under conditions that completely blocked the expulsion of the MDR substrate Rhodamine 123, did not affect delivery of either lipid analogue to the lumenal leaflet of BC as judged by the ability of sodiumdithionite to reduce the entire pool of BC-associated NBD fluorescence (Fig. 7 *A*; compare with van IJzendoorn et al., 1997). This implies that the analogues reached the apical membrane by vesicular transport, the NBD-tagged lipids residing in the inner leaflet of the vesicular membrane. Note that NBD fluorescence, had it been located in the cytoplasmic leaflet of the BC membranes, in contrast to that with a lumenal orientation, would not be accessible to quenching by sodiumdithionite under the experimental conditions (see Materials and Methods; compare with Fig. 4). Therefore, the presence of any NBD fluorescence in the cytoplasmic BC leaflet resulting from impaired translocator activity would have prompted us to classify such BC as NBD-positive. Identical results were obtained when the cells had been preincubated with MK 571 (compare with Fig. 7 *A*), a specific inhibitor of the function of basolaterally located MRP1, which has been shown to partly overlap with the exclusively at the BC membrane localized MDR1 (Roelofsen et al., 1997). Thus neither MDR1 nor MRP1 were involved in the delivery of $C_6$-NBD-GlcCer and $C_6$-NBD-SM to the lumenal leaflet of BC.

It is then reasonable to assume that subsequent transport from apical membrane to SAC is vesicle mediated, delivering the exoplasmic lipids to the inner leaflet of the SAC. Indeed, given the capacity of the analogues to readily engage in monomeric transfer and yet, their specific retainment in SAC at 18°C, the data are entirely consistent with a localization that is restricted to the inner leaflet of SAC membranes. Subsequent transport after sorting in this compartment most likely occurred by a vesicle-mediated mechanism. This was inferred from the following experiments. Monomeric trafficking from SAC would have resulted in a preferential delivery of $C_6$-NBD-GlcCer to the cytoplasmic leaflet of the apical membrane and of $C_6$-NBD-SM to the corresponding leaflet of the basolateral membrane. The subsequent appearance at the exoplasmic leaflet would then require translocation via MDR1 and MRP1, respectively. To investigate whether any fraction of the lipid analogues that had left the apical membrane could reach the inner leaflet of the basolateral PM, and thus become susceptible to translocation by MRP1, cells were first incubated according to steps 1 and 2 (see Fig. 1). MK 571 was added during step 2. The cells were then rewarmed to 37°C and further incubated in HBSS, supplemented with BSA and MK 571 for 1 h. As shown in Fig. 7 *B*, the fraction of lipid analogues that could be back exchanged from the basolateral surface was similar to that of non-treated cells. Subsequently, we examined transport of SAC-accumulated lipids. Thus, the cells were treated subsequent to step 4 (i.e., before chasing the lipid analogues from the SAC), with either PSC 833 or MK 571. However, in neither case did the treatment affect the preferential trafficking of $C_6$-NBD-GlcCer and $C_6$-NBD-SM

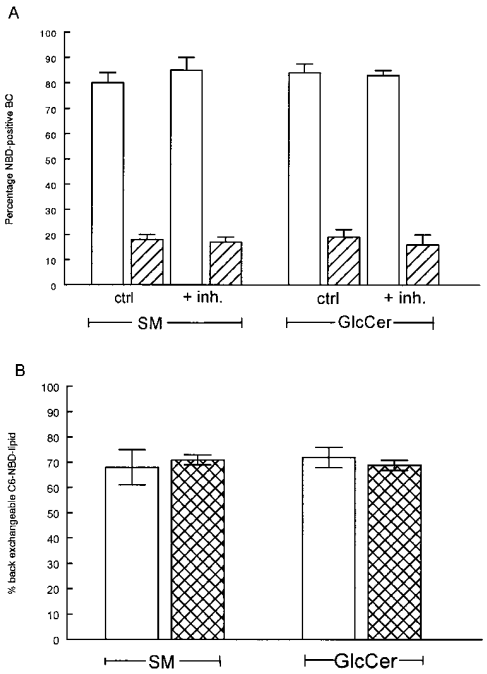


*Figure 7.* Multi-drug resistance proteins, MDR1 and MRP1, do not affect $C_6$-NBD-lipid arrival at the PM domains. In *A*, cells were preincubated with PSC 833 (5 μg/ml) at 37°C for 30 min before step 1 (see Fig. 1). In the presence of the drug, the cells were then labeled with lipid analogues at 37°C for 30 min. The cells were subsequently subjected to a back exchange (step 2 of Fig. 1) and the percentage of NBD-positive BC was determined (*white bars*). Alternatively, cells were subsequently treated with 30 mM dithionite and the percentage of NBD-positive BC was determined (*hatched bars*). In *B*, cells were incubated with either lipid analogue at 37°C for 30 min and back exchanged at 4°C twice for 30 min. Then, cells were rewarmed to 37°C and incubated for 1 h in back exchange medium. Lipids were extracted from the back exchange media and cell fractions to determine the percentage back exchangeable $C_6$-NBD-lipid. Data are expressed as mean ± SEM of at least two independent experiments.

to the apical or basolateral PM domain, respectively (compare with Fig. 5). Taken together, the results indicate that $C_6$-NBD-SM and $C_6$-NBD-GlcCer were not used as a substrate for the multi-drug resistance proteins at either PM domain and therefore must have been residing in the lumenal leaflet of vesicular compartments during all transport steps. Hence, the observed sorting of $C_6$-NBD-SM and $C_6$-NBD-GlcCer must have been restricted to the lumenal leaflet of the SAC.

### *Transcytosing pIgR-IgA Colocalizes with Apically Derived $C_6$-NBD-Sphingolipids in the SAC*

In MDCK cells, SAC (also referred to as ARC) have been described that are part of the transcytotic pathway, as revealed by the trafficking of the pIgR-IgA receptor–ligand complex, an established transcytotic marker (Apodaca et al., 1994; Barosso and Sztul, 1994). To further define the identity of the SAC through which both $C_6$-NBD-SM and $C_6$-NBD-GlcCer pass, the intracellular trafficking of fluorescently labeled IgA in HepG2 was examined, and related to that of the lipid analogues. HepG2 cells do not endogenously express the pIgR. Consistently, we were unable to detect pIgR by indirect immunofluorescence using an anti-pIgR mAb (not shown). However, some internalization of TxR-IgA was observed. Yet, this uptake could be completely abolished by adding excess asialofetuin (not shown), indicating that in HepG2 cells IgA can presumably also become internalized by the asialoglycoprotein receptor, consistent with previous observations (Tomana et al., 1988). We therefore stably transfected HepG2 cells with the pIgR (see Materials and Methods), which at steady-state was distributed throughout the cytoplasm with a preference for the apical region of the cell, and monitored the internalization of IgA in the presence of excess asialofetuin. When cells were incubated with 50 μg/ml TxR-IgA at 4°C for 30 min, washed, and then incubated at 37°C for short time intervals only (20 min or less), a substantial fraction of the intracellular fluorescence could already be detected in SAC (Fig. 8 *a*). Prolonged incubations at 37°C (Fig. 8 *b*), but not 18°C (Fig. 8 *c*), resulted in a pronounced labeling of BC, indicating that pIgR-IgA traveled through SAC before being delivered to BC. Moreover, the delivery of sub-apically located pIgR-IgA to BC was impaired at 18°C. To determine whether the TxR-IgA–labeled SAC were the same as those in which apically derived lipid analogues were found to accumulate (i.e., SAC [see Fig. 2, *d* and *f*]), cells were incubated with TxR-IgA at 4°C for 30 min, washed, and then incubated with $C_6$-NBD-SM at 37°C, allowing both compounds to enter the cells. After a back exchange of the fluorescent lipid pool associated with the basolateral PM (see Fig. 1, *step 2*), $C_6$-NBD-SM was found to label intracellular vesicular structures and BC (compare with Fig. 2, *c* and *d*; van IJzendoorn et al., 1997). Note that pretreatment with excess asialofetuin did not affect uptake and intracellular localization of the lipid analogue (not shown). In the same cells, TxR-IgA was detected in both BC and vesicular structures located near the BC (Fig. 8 *a*). The cells, thus containing intracellular pools of IgA and sphingolipid, were subsequently incubated at 18°C for 1 h to allow apically derived lipid analogues to accumulate in SAC as described above. Interestingly, as evidenced by confocal laser scanning microscopy, TxR-IgA distribution displayed a substantial overlap with $C_6$-NBD-SM in the SAC (Fig. 8, *d–g*, *arrows*). Similar results were obtained with $C_6$-NBD-GlcCer and $C_6$-NBD-GalCer (not shown). Note that the data in Fig. 8 demonstrate a colocalization of lipid and IgA, particularly in the prominently present SAC. Some differences in localization of lipid analogue and IgA can be readily explained by the notion that the lipid is transported from BC to SAC, whereas IgA enters SAC, arriving from the basolateral membrane. Also, the fate of the subsequent flow differs, SM traveling to the basolateral

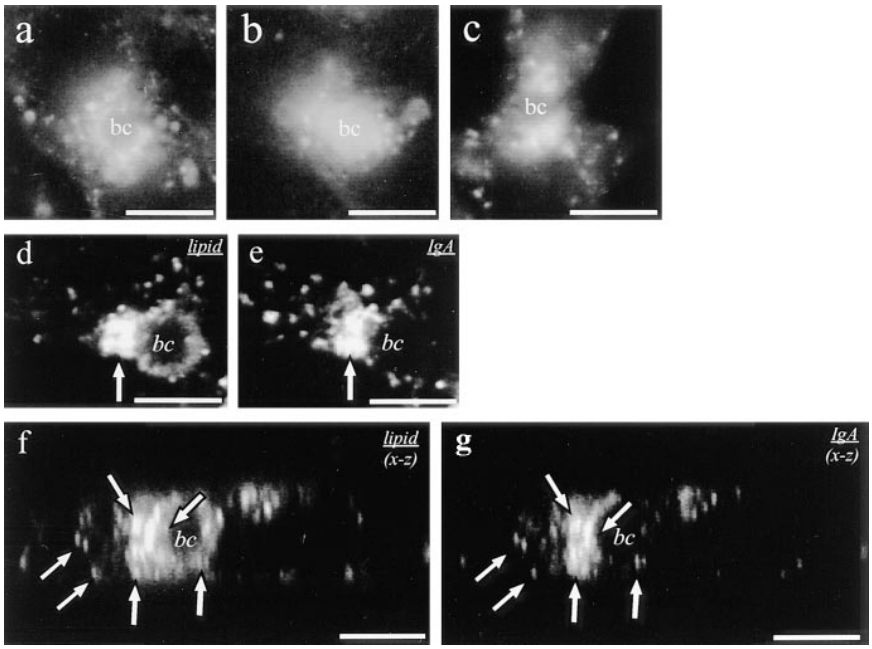


*Figure 8.* Transcytosing IgA and NBD-labeled sphingolipids colocalize in SAC in HepG2 cells. Asialofetuin-pretreated cells were labeled with 50 μg/ml TxR-IgA at 4°C for 30 min, washed, and then incubated at 37°C for 20 min in HBSS (*a*). The cells were further incubated at 37°C for another 30 min (*b*) or alternatively, cooled to 18°C and further incubated at this temperature for 60 min (*c*). In *d–g*, confocal images of the BC area, labeled with $C_6$-NBD-lipid (*d* and *f*) or TxR-IgA (*e* and *g*) are shown (*f* and *g*, x-z sections of *d* and *e*, respectively). Note the similarity in the shape of the fluorescence pattern obtained for accumulating protein and lipid, adjacent to the BC (*arrows*). Bar, 5 μm.

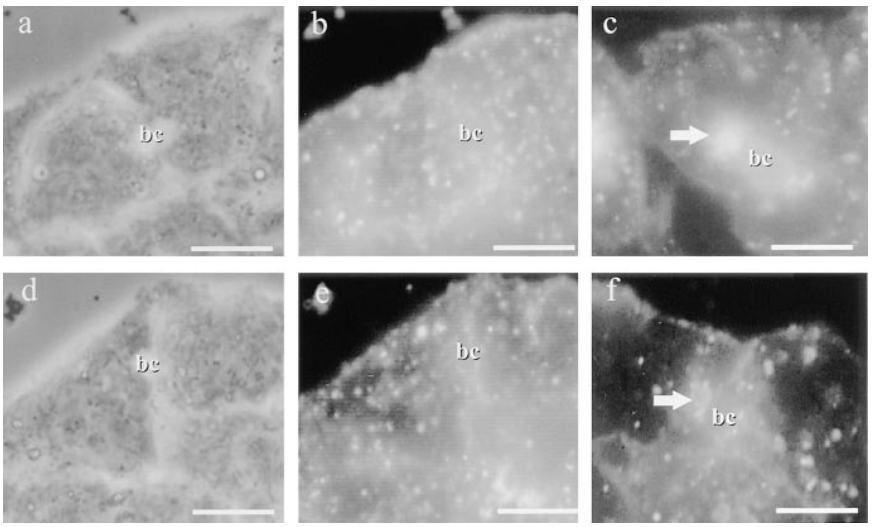


*Figure 9.* Nocodazole prevents accumulation of $C_6$-NBD-lipids in the SAC. Cells were labeled and treated according to steps 1 and 2 of Fig. 1. During step 2, 33 μM nocodazole was included to disrupt the cell its microtubules. In the presence of nocodazole, the cells were then incubated at 18°C for 1 h in back exchange medium, washed, and then photographed. Note the absence of accumulation of $C_6$-NBD-SM (*b*; *a*, phase contrast to *b*) and $C_6$-NBD-GlcCer (*e*; *d*, phase contrast to *e*) in the sub-apical area (for control, see Fig. 2). Sub-apical labeling reappeared after a prolonged incubation in back exchange medium at 37°C for 60 min, in the absence of nocodazole (*arrows*: *c*, $C_6$-NBD-SM; *f*, $C_6$-NBD-GlcCer). Bar, 10 μm.

membrane, whereas IgA travels to the apical membrane (see also Discussion). In conclusion, the results indicate that the sorting compartment for simple monohexoylsphingolipids in the reverse transcytotic pathway in HepG2 cells, SAC, displays the same identity as pIgR-IgA–accumulating compartments identified in MDCK as ARC.

### *Transport of Apically Derived $C_6$-NBD-GlcCer and -SM to SAC, but Not Apical Endocytosis of $C_6$-NBD-GlcCer and -SM Is Affected by Nocodazole*

The aforementioned results indicate that the mechanism of sphingolipid trafficking between apical membrane and SAC, is accomplished by vesicular transport. Many vesicular transport events appear to require an intact microtubule network. To investigate the involvement of microtubules in transport between the apical PM and the SAC, cells were incubated with $C_6$-NBD-SM or -GlcCer at 37°C for 30 min, after which the pool of fluorescent lipid analogues in the basolateral PM was depleted with BSA (Fig. 1, *step 1* and *2*). During this back exchange procedure 33 μM nocodazole was included, a concentration sufficient to disrupt microtubules as revealed by immunofluorescence using a mAb directed against β-tubulin (not shown). After extensive washing, the cells were incubated at 18°C and BC-associated lipid analogues were chased in back exchange medium (HBSS + 5% BSA), supplemented with nocodazole for 1 h. Internalization of either lipid analogue from the apical PM was not inhibited by nocodazole, as judged by the similarities in the decrease of the percentage of NBD-labeled BC, when compared with non-treated cells (Table I). However, whereas in non-treated cells, intensely labeled SAC was observed after a 1-h chase at 18°C (Fig. 2, *d* and *f*), in nocodazole-treated cells the labeling of SAC was conspicuously absent. Rather, numerous small vesicular structures, labeled with either $C_6$-NBD-SM or -GlcCer, were seen, distributed throughout the cytoplasm (Fig. 9, *a–d*). The effect of nocodazole was reversible, and $C_6$-NBD-GlcCer– and -SM–labeled SAC appeared after a prolonged incubation in nocodazole-free medium (Fig. 9, *c* and *f*, *arrows*). Concomitantly, immunofluorescence experiments to visualize β-tubulin (as described above) revealed that intact microtubules reappeared during this prolonged incubation (not shown).

Previously, it was demonstrated that the organization of the sub-apical compartments (ARC) as described in MDCK cells requires an intact microtubule network. Thus, whereas the SAC in control cells were concentrated in a centralized spot, they were found to be dispersed throughout the apical cytoplasm in the nocodazole-treated cells (Apodaca et al., 1994). To investigate whether the organization of the SAC, as shown in Figs. 2 (*d* and *f*) and 4, was also dependent on intact microtubules, SAC were first pre-loaded with either lipid analogue by chasing BC-associated lipid at 18°C for 1 h as described above. After quenching of label in BC with dithionite (Fig. 1, *step 4*), the cells were incubated in nocodazole-containing HBSS at 4°C or 18°C for 1 h. Although the microtubule organization was effectively disrupted at either condition (see above), nocodazole did not change the appearance of labeled SAC, implying that their appearance was indistinguishable from that in non-treated cells (Fig. 10, *a* and *b*). However, under identical experimental conditions, nocodazole was found to be effective in disrupting $C_6$-NBD-Cer–preloaded Golgi apparatus (Fig. 10, *c* and *d*; Turner and Tartakoff, 1989). The results thus indicate that rather than (early) apical endocytosis or the organization of the

*Table I. Effect of Nocodazole on the Disappearance of $C_6$-NBD-SM and $C_6$-NBD-GlcCer from BC*

| | Percent of NBD-positive BC | |
|---|---|---|
| | $C_6$-NBD-GlcCer | $C_6$-NBD-SM |
| Before chase | 100 | 100 |
| After chase | | |
| control | 61 ± 5 | 59 ± 4 |
| nocodazole | 58 ± 2 | 57 ± 3 |

Cells were incubated with $C_6$-NBD-GlcCer or -SM at 37°C for 30 min. The fluorescent pool of $C_6$-NBD-lipids in the basolateral PM was then back exchanged in the absence or presence of nocodazole. Cells were then rewarmed to and further incubated in back exchange medium with or without nocodazole at 18°C for 1 h. The percentage of NBD-positive BC (i.e., BC alone and BC + SAC) was determined as described in Materials and Methods. The percentage of NBD-positive BC before the chase was set at 100%. Data are expressed as mean ± SEM of at least two independent experiments.

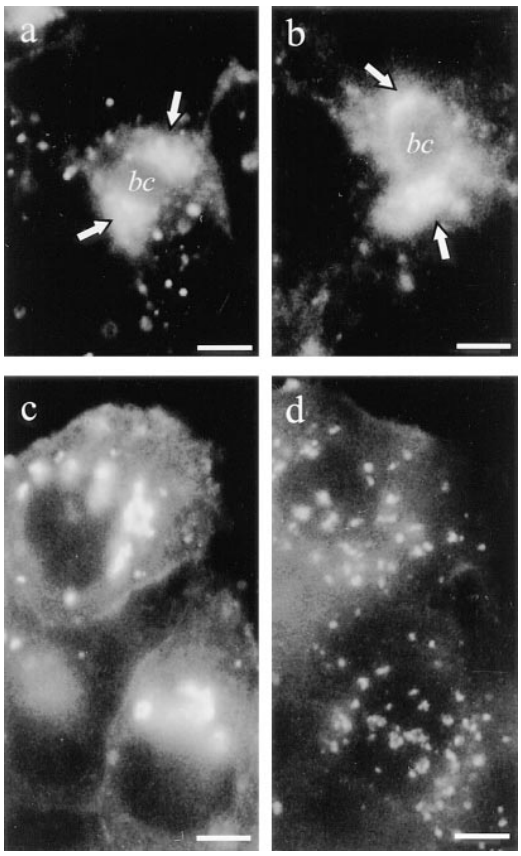


*Figure 10.* Nocodazole does not affect the spatial organization of SAC but perturbs the organization of the Golgi apparatus. In *a* and *b*, cells were labeled with $C_6$-NBD-GlcCer according to steps 1–4 of Fig. 1, to label SAC. In *b*, cells were subsequently incubated with 33 μM nocodazole at 4°C for 60 min. Note that nocodazole does not affect the appearance of the NBD lipid–labeled SAC. This was also the case when the nocodazole-treatment was done at elevated temperatures (van IJzendoorn, S.C.D., and D. Hoekstra, unpublished observations). In *c* and *d*, cells were labeled with 4 μM $C_6$-NBD-Cer at 4°C for 30 min, washed, and then incubated in back exchange medium at room temperature for 20 min. A typical Golgi apparatus labeling pattern was obtained (*c*). In parallel, such Golgi-labeled cells were subsequently treated with 33 μM nocodazole at 4°C for 60 min (*d*). Note the clearly different fluorescence pattern in the nocodazole-treated cells. Bar, 5 μm.

SAC, (a) distinct transport step(s) after endocytic internalization, but before the delivery to SAC, is dependent on intact microtubules.

## *Discussion*

In polarized HepG2 cells, the sphingolipid analogues $C_6$-NBD-GlcCer and $C_6$-NBD-SM display a preferential plasma membrane localization, the GlcCer derivative accumulating primarily at the apical membrane, while the SM derivative prefers the basolateral membrane (van IJzendoorn et al., 1997). The mechanism underlying this preferential distribution involves their internalization from the apical, BC surface. For the trafficking of GlcCer, a tentative role for a non-Golgi–related compartment was

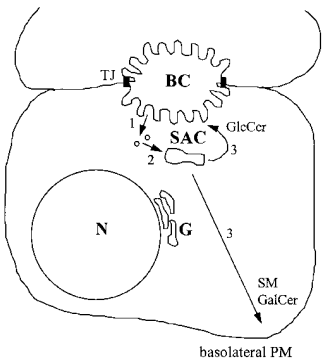


*Figure 11.* The role of SAC in the trafficking/sorting of sphingolipids in the apical to basolateral transcytotic pathway in HepG2 cells. $C_6$-NBD-sphingolipids are endocytosed from the apical, bile canalicular plasma membrane (step *1*) and transported to SAC via a route of which at least part is microtubule dependent (step *2*). Exit from the SAC (step *3*) appears to be temperature dependent as it can be blocked at 18°C. Note that the spatial organization of SAC does not require an intact microtubule network (see text). In the SAC, presumably within its lumenal leaflet, the sphingolipids are sorted, followed by vesicular transport of $C_6$-NBD-GlcCer, preferentially to the apical plasma membrane domain, and of $C_6$-NBD-SM and $C_6$-NBD-GalCer, preferentially to the basolateral plasma membrane domain (step *3*). *SAC*, sub-apical compartments; *BC*, bile canalicular plasma membrane; *N*, nucleus; *G*, Golgi apparatus; *TJ*, tight junctional complex.

proposed. In the present study, we have established the identity of these compartments and their functional involvement in determining the distinct fate of several sphingolipids in the apical to basolateral pathway. Furthermore, the data demonstrate that the processing of $C_6$-NBD-GlcCer and $C_6$-NBD-SM in HepG2 cells is accomplished by vesicular transport and that the preferential localization in either plasma membrane domain is not mediated by interference of multi-drug resistance proteins, which have been reported to display the ability to translocate lipid analogues from inner to outer leaflet across plasma membranes (van Helvoort et al., 1997). Rather, after having reached the apical membrane by transcytosis, after initial insertion in the basolateral membrane, the lipid analogues were transported from the BC toward SAC, where they accumulate at low (18°C) temperature, reflecting a temperature-sensitive step in the exit of the lipids from this compartment. In Fig. 11, a model depicting the central involvement of SAC in apical to basolateral transcytosis of sphingolipids in HepG2 cells is presented. In this figure, transport of the sphingolipids from BC to SAC is represented by steps 1 and 2. Transport to the SAC is microtubule dependent (Fig. 11, step *2*) and represents a direct pathway, i.e., it does not involve trafficking via the basolateral PM, as the presence of BSA in the incubation medium precludes any re-uptake and subsequent trafficking of the lipids back to the apical pole. The results indicate that SAC constitute an intrinsic part of the apical to basolateral transcytotic pathway through which (glyco)sphingolipids traverse the cells, bearing reminiscence of a sub-apical compartment, previously identified as ARC in polarized protein transport in MDCK cells (Apodaca et al., 1994; Barosso and Sztul, 1994). However, an important distinction between both compartments is that the structural organization of ARC depends on an intact microtubule system, in marked contrast to SAC, the integrity of which does not depend on microtubules. In this Golgi-unrelated compartment, lipid sorting occurs, implying that GlcCer is

recycled to the apical membrane, whereas NBD derivatives from SM and GalCer are processed by vesicular transport to the basolateral membrane (Fig. 11, step *3*). Hence, SAC appear to play a prominent role in maintaining lipid polarity in polarized hepatic cells.

### *Characteristics of the SAC*

The identity of SAC as a compartment specifically associated with the transcytotic pathway in HepG2 cells, is supported by the observation that the transcytotic marker IgA/pIgR traverses this compartment in a temperature-dependent manner. In polarized MDCK cells, its validity as a transcytotic marker has been demonstrated, and low temperature inhibits transcytosis of receptor-bound IgA by an impaired exit of this receptor–ligand complex from structures located near the apical PM, i.e., ARCs. Indeed, inhibitory effects of low temperature on transcytotic transport of proteins in polarized cells, without affecting endocytosis, have been shown before (Maratos-Flier, 1987; Breitfeld et al., 1989; Hunziker and Mellman, 1989; Apodaca et al., 1994; Barosso and Sztul, 1994). Moreover, IgA- and transcytosing pIgR–containing vesicular structures located subjacent the apical PM have been described in rat hepatic cells (Hoppe et al., 1985; Barr and Hubbard, 1993; Geuze et al., 1984; Hemery et al., 1996) and in polarized WIF-B cells (Ihrke et al., 1998). HepG2 cells are of human origin and do not express the pIgR. Expression was accomplished however by transfection and transfected HepG2 cells were found to internalize TxR-IgA, which was rapidly transported to the apical pole (Fig. 8 *a*), consistent with the anticipated fate of a transcytotic marker. Interestingly, whereas intense labeling of BC was observed after longer incubations at 37°C (Fig. 8 *b*), TxR-IgA was not fully transcytosed to the apical surface at 18°C but accumulated in SAC instead. Since TxR-IgA was observed in SAC before it appeared in the BC, the data suggest that SAC-associated TxR-IgA originated directly from the basolateral area rather than from the apical PM from which IgA (at least in rat hepatocytes) can be internalized (Jones et al., 1984). This conclusion is entirely compatible with the fate of pIgR in hepatic WIF-B cells (Ihrke et al., 1998). Importantly, apically derived $C_6$-NBD-lipids were found to colocalize with transcytosing TxR-IgA in the SAC (Fig. 8, *d* vs. *e*, and *f* vs. *g*). Remarkably, in contrast to *apically* derived $C_6$-NBD-lipids, which were found to colocalize with transcytosing TxR-IgA in SAC (Fig. 8, *d–g*), *basolaterally* derived lipid was far less prominently trapped in SAC at 18°C. As demonstrated before, basolateral to apical trafficking of the sphingolipids proceeds by bulk flow, whereas segregation is seen in the apical to basolateral pathway (van IJzendoorn et al., 1997). The appreciation of the involvement of SAC in apically directed bulk flow trafficking of the lipid analogues therefore remains to be determined. The data emphasize however the involvement of SAC as a sorting compartment in the segregation of the lipids, as occurs in the reverse pathway. Thus, the striking similarity with respect to the intracellular (sub-apical) localization and the temperature-dependent characteristics concerning the trafficking of IgA via these compartments supports the view, that the lipid-labeled SAC in HepG2 cells and the ARC in MDCK cells are analogous. Ihrke et al. (1998) proposed that SAC in hepatic WIF-B cells are mainly a one-way sorting station in the basolateral to apical pathway, as they were unable to detect recycling resident apical proteins in similar SAC by biochemical means (Barr and Hubbard, 1993; Barr et al., 1995). However, our experiments, in which we are able to directly monitor the endocytic flow of apical membrane in living cells, indicate that the transcytotic trafficking pathways between apical and basolateral membranes and vice versa do appear to merge in SAC. The relationship between lipid and protein traffic via these compartments is clearly an important issue that needs to be addressed in future studies.

Golgi markers are excluded from the apical recycling compartments in MDCK cells, and an (apical) endosomal nature of the compartment was proposed (Apodaca et al., 1994). Two pieces of evidence indicate that also in HepG2 cells SAC appear to be unrelated to the Golgi apparatus. First, whereas monensin inhibits sphingolipid transport from the Golgi-apparatus to BC in HepG2 cells (van IJzendoorn et al., 1997) as well as to the PM in non-polarized cells (Lipsky and Pagano, 1985; Kok et al., 1992), apical to basolateral transcytosis of $C_6$-NBD-GlcCer and $C_6$-NBD-SM in HepG2 cells is unaffected by this treatment. Second, treatment of the cells with nocodazole, a microtubule-disrupting compound, clearly affected the morphology of the Golgi apparatus, but had no visible effect on the morphology of SAC preloaded with fluorescent lipid analogue (Fig. 10). Intriguingly however, this very feature distinguishes SAC from ARC in MDCK cells in that the integrity of the latter entirely depends on an intact microtubular organization (Apodaca et al., 1994).

Interestingly, nocodazole inhibited transport of lipid analogues from BC to SAC (Fig. 9), but not apical endocytosis (Table I; Fig. 11, steps *1* and *2*). Transport of proteins and lipids from the PM to early "sorting" endosomes is typically microtubule-independent (Hunziker et al., 1990; Matter et al., 1990; Kok et al., 1992). By contrast, transport of proteins and lipids from such early sorting endosomes to a functionally and morphologically distinct set of endosomal compartments located in the perinuclear region (Gruenberg and Maxfield, 1995) requires an intact microtubule network (Gruenberg et al., 1989; Hunziker et al., 1990; Kok et al., 1992). Moreover, the ARC appears to share a striking homology with the perinuclear recycling endosome, described in non-polarized cells (Zacchi et al., 1998). These features also seem to hold for the present system, when comparing the localization of lipid analogues and pIgR in polarized and non-polarized HepG2 cells (Fig. 2, see below). Hence, in conjunction with its localization in the juxtanuclear/Golgi area facing the apical PM (Gruenberg and Maxfield, 1995), SAC thus bear reminiscence to a recycling endosomal compartment rather than to an early sorting endosome, correlating with the pericentriolar localization of recycling endosomes in other polarized cells (Hughson and Hopkins, 1990). Obviously, a detailed characterization of the localization of specific markers (e.g., mannose-6-phosphate receptor; different rab proteins, etc.) will be required to obtain further insight into the exact nature of this compartment. However, given that apical membrane derived lipid analogues and basolateral membrane derived IgA are both delivered to SAC

(Fig. 8), it would thus appear that the compartment acts as a "traffic center" in (reverse) transcytotic trafficking in polarized cells. Fully compatible with this conclusion is a previous hypothesis that pathways originating from the apical and basolateral pathways merge at a perinuclear endosomal compartment that is distinct from early (sorting) endosomes in polarized cells (Parton et al., 1989; Hughes and Hopkins, 1990).

Intriguingly, accumulation of the lipid analogues and IgA was also observed in non-polarized HepG2 cells, i.e., cells that had not formed an apical, biliary PM domain. This accumulation was typically in the juxtanuclear area of the cells (Fig. 2, *wide arrows*), and was abolished in nocodazole-pretreated cells (Fig. 9), similarly as observed for sphingolipid transport from early to perinuclear endosomes in non-polarized BHK cells (Kok et al., 1992). These observations underscore that SAC is not a unique compartment, but rather that its specific functional features, including sorting in (reverse) transcytosis, are becoming apparent only in polarized cells. Indeed, after submission of this manuscript, Zacchi et al. (1998) reported that rab17, a small GTPase that has been shown to be induced upon cell polarization (Lütcke et al., 1993), associates with both the ARC in polarized cells and the perinuclear recycling endosome when expressed in non-polarized cells.

### *Sorting of Sphingolipids in SAC*

After treatment with sodiumdithionite, NBD fluorescence in BC, but not in SAC, was nearly completely eliminated (Figs. 4 and 5, *B* and *C*, *0 min*; compare with van IJzendoorn et al., 1997). This approach thus allows to monitor subsequently the fate of the lipid analogues that have accumulated into SAC (at 18°C). Indeed, after a 30-min chase at 37°C, the extent of BCP labeling with $C_6$-NBD-SM or $C_6$-NBD-GalCer had decreased by >30% and 20%, respectively, compared with that with $C_6$-NBD-GlcCer (Figs. 5 *A* and 6 *A*). This indicated that $C_6$-NBD-SM and $C_6$-NBD-GalCer, relative to $C_6$-NBD-GlcCer, were transported out of the bile canalicular region (Fig. 5 *A* and 6 *A*). Indeed, whereas the fractions of both SM and GalCer that remained in the BCP area were primarily restricted to SAC, that of GlcCer showed a different fate. Not only did the latter lipid show a strong preference for a localization in the apical region of the cell, as reflected by the fact that ~90% of the BCP remained labeled with this lipid during a chase of at least 30 min, there was also an apparent trend of its time-dependent translocation from SAC to the BC. Evidently, these kinetic changes in pool size and BCP localization (SAC versus BC) are entirely consistent with the preferential localization of GlcCer in the apical and that of SM in the basolateral region of the cell (van IJzendoorn et al., 1997). Here, we show that GalCer also shows a distinct preference for a basolateral localization, although less pronounced than SM. The results indicate that SAC determine the subsequent fate of the lipid analogues, involving their flow from the SAC to preferential PM domains, and implying that sorting occurs in these compartments.

Presumably, segregation of the sphingolipids takes place within the lumenal leaflet of the SAC, since inhibitors of MDR1/P-glycoprotein and MRP1, previously shown to be able to translocate $C_6$-NBD-lipids over the PM (van Helvoort et al., 1996), did not affect the outcome of the experiments (Fig. 7). Hence, monomeric trafficking to the inner leaflet of either plasma membrane, followed by outward translocation by either MDR1 or MRP1, can be excluded. Thus, a highly specific sorting event, given the remarkable distinction that becomes apparent in the sorting of GlcCer and its epimer, GalCer, and vesicular packaging underlie the overall processing of the lipid analogues by SAC. In this context it is interesting to mention that the calmodulin antagonist W7 appears to have distinct effects on the trafficking of $C_6$-NBD-GlcCer and $C_6$-NBD-SM from the SAC, thus supporting the proposed model in which GlcCer and SM are segregated into distinct pools within the SAC membranes, which can be separately recognized by mechanisms that regulate trafficking (van IJzendoorn, S.C.D., and D. Hoekstra, unpublished results).

In the biosynthetic pathway, apical sorting in polarized cells has mainly focused on a mechanism involving targeting of glycosphingolipid-enriched clusters or rafts, originating from the TGN (Simons and Ikonen, 1997; Weimbs et al., 1997). In addition, glycosphingolipid-enriched rafts were also postulated to be involved in endocytotic and transcytotic transport routes, mediated by caveolae. In the present study, we present for the first time evidence that clearly indicates a role for a non-Golgi–related intracellular compartment in the sorting and, consequently, polarized distribution of sphingolipids. However, the ubiquity of this phenomenon remains to be determined, the site and extent of sorting being dependent on cell type and nature of transport route (biosynthetic pathway, basolateral to apical membrane flow, i.e., transcytosis, or the reverse pathway). For example, sphingolipid sorting in the transcytotic pathway could not be demonstrated in MDCK cells (van Genderen and van Meer, 1995). Possibly, sorting of sphingolipids in this pathway is restricted to hepatic cells, which are thought to rely heavily on transcytosis for the correct targeting and delivery of apical proteins (Bartles et al., 1987; Schell et al., 1992). It is yet of interest however, that in MDCK cells, $C_6$-NBD-GlcCer and $C_6$-NBD-SM, endocytosed from either PM domain reach the apical recycling compartments, where they colocalize with the IgA/pIgR complex, before delivery to the opposite surface (van IJzendoorn, S.C.D., K.E. Mostov, and D. Hoekstra, manuscript in preparation). In MDCK cells, sorting of newly synthesized sphingolipids is believed to occur predominantly in the biosynthetic pathway and the actual sorting compartment was proposed to be the TGN (Simons and van Meer, 1988). Although newly synthesized $C_6$-NBD-GlcCer and $C_6$-NBD-SM can be directly transported to either PM domain in HepG2 cells (Zaal et al., 1994; Zegers and Hoekstra, 1997), sorting of sphingolipids has not been demonstrated in hepatic cells yet. Also, the direct Golgi to apical transport pathway is poorly characterized and the intriguing question remains as to whether SAC are part of this route in HepG2 cells. Further research is imperative for a better understanding of the functional involvement of the SAC/ARCs in the different polarized cell types with respect to lipid trafficking in distinct transport routes as well as the integration of lipid and protein trafficking. Such work is currently in progress in our laboratory. The identification in HepG2 cells of a non-

Golgi–related intracellular compartment, SAC, that is involved in the trafficking and sorting of sphingolipids and, moreover, its similarity to the ARC in MDCK cells (Apodaca et al., 1994), will be of great importance to further reveal and understand mechanisms underlying the generation and maintenance of membrane polarity.

We wish to thank Dr. K. Mostov for his kind gift of pIgR cDNA and anti-pIgR antibody; Dr. K. Dunn for kindly providing us with TxR-labeled IgA; Dr. E. Vellenga for the PSC833 and MK 571; Dr. H. Roelofsen for advice and assistance with confocal laser scanning microscopy; P.v.d. Syde and D. Huizinga for photographical work, and W. Visser for expert technical assistance with the transfections. We thank Drs. K. Mostov, J.W. Kok, and M. Zegers for helpful and stimulating discussions.

Received for publication 19 February 1998 and in revised form 29 June 1998.

### *References*

Ali, N., and W.H. Evans. 1990. Priority targeting of gucosyl-phosphatidylinositol-anchored proteins to the bile canalicular (apical) plasma membrane of hepatocytes. *Biochem. J.* 271:193–199.

Apodaca, G., M. Bomsel, J. Arden, P.P. Breitfeld, K. Tang, and K.E. Mostov. 1991. The polymeric immunoglobulin receptor: a model protein to study transcytosis. *J. Clin. Invest.* 87:1877–1882.

Apodaca, G., L.A. Katz, and K.E. Mostov. 1994. Receptor mediated endocytosis of IgA in MDCK cells is via apical recycling endosomes. *J. Cell Biol.* 125: 67–86.

Babia, T., J.W. Kok, and D. Hoekstra. 1994. The use of fluorescent lipid analogues to study endocytosis of glycosphingolipids. *In* Receptor Research Methods. B. Greenstein, editor. Harwood Academic Publishing, London. 155–174.

Barosso, M., and E.S. Sztul. 1994. Basolateral to apical transcytosis in polarized cells is indirect and involves BFA and trimeric G protein sensitive passage through the apical endosome. *J. Cell Biol.* 124:83–100.

Barr, V.A., and A.L. Hubbard. 1993. Newly synthesized hepatocyte plasma membrane proteins are transported in transcytotic vesicles in the bile ductligated rat. *Gastroenterology.* 105:44–571.

Barr, V.A., L.J. Scott, and A.L. Hubbard. 1995. Immunoadsorption of hepatic vesicles carrying newly synthesized dipeptidyl peptidase IV and polymeric IgA receptor. *J. Biol. Chem.* 270:27834–27844.

Bartles, J.R., H.M. Feracci, B. Stieger, and A.L. Hubbard. 1987. Biogenesis of the rat hepatocyte plasma membrane in vivo: Comparison of the pathways taken by apical and basolateral proteins using subcellular fractionation. *J. Cell Biol.* 105:1241–1251.

Bligh, E.G., and W.J. Dyer. 1959. A rapid method of total lipid extraction and purification. *Can. J. Biochem. Biophys.* 37:911–1017.

Breitfeld, P.P., J.M. Harris, and K.E. Mostov. 1989. Postendocytic sorting of the ligand for the polymeric immunoglobulin receptor in Madin-Darby canine kidney cells. *J. Cell Biol.* 109:475–486.

Brown, D.A., and J.K. Rose. 1992. Sorting of GPI-anchored proteins to glycolipid-enriched membrane subdomains during transport to the apical surface. *Cell.* 68:533–544.

Cariappa, R., and M.S. Kilberg. 1992. Plasma membrane domain localization and transcytosis of the glucagon-induced hepatic system A carrier. *Am. J. Physiol.* 263:1021–1028.

Geuze, H.J., J.W. Slot, G.J.A.M. Strous, J. Peppard, K. von Figura, A. Hasilik, and A.L. Schwartz. 1984. Intracellular receptor sorting during endocytosis: comparative immunoelectron microscopy of multiple receptors in rat liver. *Cell.* 37:195–204.

Goda, S., T. Kobayashi, and I. Goto. 1987. Hydrolysis of galactosylsphingosine and lactosylsphingosine by β-galactosidases in human brain and cultured fibroblasts. *Biochim. Biophys. Acta.* 920:259–265.

Gruenberg, J., and F.R. Maxfield. 1995. Membrane transport in the endocytic pathway. *Curr. Opin. Cell Biol.* 7:552–563.

Gruenberg, J., G. Griffiths, and K.E. Howell. 1989. Characterization of the early endosome and putative endocytic carrier vesicles in vivo and with an assay of vesicle fusion in vitro. *J. Cell Biol.* 108:1301–1316.

Hemery, I., A. Durand-Schneider, G. Feldmann, J. Vaerman, and M. Maurice. 1996. The transcytotic pathway of an apical plasma membrane protein (B10) in hepatocytes is similar to that of IgA and occurs via a tubular pericentriolar compartment. *J. Cell Sci.* 109:1215–1227.

Hoppe, C.A., T.P. Connolly, and A.L. Hubbard. 1985. Transcellular transport of polymeric IgA in the rat hepatocyte: Biochemical and morphological characterization of the transport pathway. *J. Cell Biol.* 101:2113–2123.

Hughson, E.J., and C.R. Hopkins. 1990. Endocytic pathways in polarized Caco-2 cells: Identification of an endosomal compartment accessible from both apical and basolateral surfaces. *J. Cell Biol.* 110:337–348.

Hunziker, W., and I. Mellman. 1989. Expression of macrophage-lymphocyte Fc receptors in Madin-Darby canine kidney cells: Polarity and transcytosis differ for isoforms with or without coated pit localization domains. *J. Cell Biol.* 109:3291–3302.

Hunziker, W., P. Male, and I. Mellman. 1990. Differential microtubule requirements for transcytosis in MDCK cells. *EMBO (Eur. Mol. Biol. Organ.) J.* 9:3515–3525.

Ihrke, G., G.V. Martin, M.R. Shanks, M. Schrader, T.A. Schroer, and A.L. Hubbard. 1998. Apical plasma membrane proteins and endolyn-78 travel through a sub-apical compartment in polarized WIF-B hepatocytes. *J. Cell Biol.* 141:115–133.

Jones AL, G.T. Hradek, D.L. Schmucker, and B.J. Underdown. 1984. The fate of polymeric and secretory immunoglobulin A after retrograde infusion into the common bile duct in rats. *Hepatology.* 4:1173–1183.

Kishimoto, Y. 1975. A facile synthesis of ceramides. *Chem. Phys. Lipids.* 15:33–36

Kok, J.W., K. Hoekstra, S. Eskelinen, and D. Hoekstra. 1992. Recycling pathways of glucosylceramide in BHK cells: distinct involvement of early and late endosomes. *J. Cell Sci.* 103:1139–1152.

Lipsky, N.G., and R.E. Pagano. 1985. Intracellular translocation of fluorescent sphingolipids in cultured fibroblasts: endogenously synthesized sphingomyelin and glucocerebroside analogues pass through the Golgi apparatus en route to the plasma membrane. *J. Cell Biol.* 100:27–34.

Lutcke, A., S. Jansson, R.G. Parton, P. Chavrier, A. Valencia, L.A. Huber, E. Lehtonen, and M. Zerial. 1993. Rab17, a novel small GTPase, is specific for epithelial cells and is induced during cell polarization. *J. Cell Biol.* 121:553–564.

Matlin, K.S., and K. Simons. 1984. Sorting of an apical plasma membrane glycoprotein occurs before it reaches the cell surface in cultured epithelial cells. *J. Cell Biol.* 99:2131–2139.

Matter, K., K. Bucher, and H.P. Hauri. 1990. Microtubule perturbation retards both the direct and the indirect apical pathway bus does not affect sorting of plasma membrane proteins in intestinal epithelial cells (Caco-2). *EMBO (Eur. Mol. Biol. Organ.) J.* 9:3163–3170.

Maratos-Flier, E., C.Y.Y. Kao, E.M. Verdin, and G.L. King. 1987. Receptor-mediated vectorial transcytosis of epidermal growth factor by Madin-Darby canine kidney cells. *J. Cell Biol.* 105:1595–1601.

Misek, D.E., E. Bard, and E. Rodriguez-Boulan. 1984. Biogenesis of epithelial cell polarity: intracellular sorting and vectorial exocytosis of an apical plasma membrane glycoprotein. *Cell.* 39:537–546.

Mostov, K.E., and D.L. Deitcher. 1986. Polymeric IgA receptor expressed in MDCK cells transcytoses IgA. *Cell.* 46:613–621.

Mostov, K.E., Y. Altschuler, S. Chapin, C. Enrich, S-H. Low, F. Luton, J. Richman-Eisenstat, K. Singer, K. Tang, and T. Weimbs. 1995. Regulation of protein traffic in polarized epithelial cells: the polymeric immunoglobulin receptor model. *Cold Spring Harbor Symp. Quant. Biol.* 60:775–781.

Parton, R.G., K. Prydz, M. Bomsel, K. Simons, and G. Griffiths. 1989. Meeting of the apical and basolateral endocytic pathways of the Madin-Darby canine kidney cell in late endosomes. *J. Cell Biol.* 109:3259–3272.

Pfeiffer, S., S.C. Fuller, and K. Simons. 1985. Intracellular sorting and basolateral appearance of the G protein of vesicular stomatitis virus in Madin-Darby canine kidney cells. *J. Cell Biol.* 101:470–476.

Roelofsen, H., T.A. Vos, I.J. Schippers, F. Kuipers, H. Koning, H. Moshage, P.L. Jansen, and M. Muller. 1997. Increased levels of the multidrug resistance protein in lateral membranes of proliferating hepatocyte-derived cells. *Gastroenterology.* 112:511–521.

Schell, M.J., M. Maurice, B. Stieger, and A.L. Hubbard. 1992. 5′ nucleotidase is sorted to the apical domain of hepatocytes via an indirect route. *J. Cell Biol.* 119:1173–1182.

Simons, K., and S.D. Fuller. 1985. Cell surface polarity in epithelia. *Annu. Rev. Cell Biol.* 1:243–288.

Simons, K., and E. Ikonen. 1997. Functional rafts in cell membranes. *Nature.* 387:569–572.

Simons, K., and G. van Meer. 1988. Lipid sorting in epithelial cells. *Biochemistry.* 27:6197–6202.

Simons, K., and A. Wandinger-Ness. 1990. Polarized sorting in epithelia. *Cell.* 62:207–210.

Tomana, M., R. Kulhavy, and J. Mestecky. 1988. Receptor-mediated binding and uptake of immunoglobulin A by human liver. *Gastroenterology.* 94:762–770.

Turner, J.R., and A.M. Tartakoff. 1989. The response of the Golgi complex to microtubule alterations: The roles of metabolic energy and membrane traffic in Golgi complex organization. *J. Cell Biol.* 109:2081–2088.

van der Woude, I., A. Wagenaar, A.A. Meekel, M.B.A. ter Beest, M.H. Ruiters, J.B. Engberts, and D. Hoekstra. 1997. Novel pyridinium surfactants for efficient, nontoxic in vitro gene delivery. *Proc. Natl. Acad. Sci. USA.* 94: 1160–1165.

van Genderen, I., and G. van Meer. 1995. Differential targeting of glucosylceramide and galactocylceramide analogues after synthesis but not during transcytosis in Madin-Darby canine kidney cells. *J. Cell Biol.* 131:645–654.

van Helvoort, A., A.J. Smit, H. Sprong, I. Fritzsche, A.H. Schinkel, P. Borst, and G. van Meer. 1996. MDR1 P-Glycoprotein is a lipid translocase of broad specificity, while MDR3 P-Glycoprotein specifically translocates phosphatidylcholine. *Cell.* 87:507–517.

van IJzendoorn, S.C.D., M.M.P. Zegers, J.W. Kok, and D. Hoekstra. 1997. Segregation of glucosylceramide and sphingomyelin occurs in the apical to basolateral transcytotic route in HepG2 cells. *J. Cell Biol.* 137:347–357.

van't Hof, W., and G. van Meer. 1990. Generation of lipid polarity in intestinal

epithelial (Caco-2) cells: Sphingolipid synthesis in the Golgi complex and sorting before vesicular traffic to the plasma membrane. *J. Cell Biol.* 111: 977–986.

Weimbs, T., S.H. Low, S.J. Chapin, and K.E. Mostov. 1997. Apical targeting in polarized epithelial cells: there's more afloat than rafts. *Trends Cell Biol.* 7:393–399.

Zaal, K.J.M., J.W. Kok, S. Sormunen, S. Eskelinen, and D. Hoekstra. 1993. Intracellular sites involved in the biogenesis of bile canaliculi in hepatic cells. *Eur. J. Cell Biol.* 63:10–19.

Zacchi, P., H. Stenmartk, R.G. Parton, D. Orioli, F. Lim, A. Giner, I. Mellman, M. Zerial, and C. Murphy. 1998. Rab17 regulates membrane traffic through apical recycling endosomes in polarized epithelial cells. *J. Cell Biol.* 140: 1039–1053.

Zegers, M.M.P., and D. Hoekstra. 1997. Sphingolipid transport to the apical plasma membrane in human hepatoma cells is controlled by PKC and PKA activity: A correlation with cell polarity in HepG2 cells. *J. Cell Biol.* 138:307–321.